ACS APPLIED MATERIALS & INTERFACES

Research Article

www.acsami.org

Electrospun Amplified Fiber Optics

Giovanni Morello,[†,‡] Andrea Camposeo,[†,‡] Maria Moffa,[†] and Dario Pisignano*[,†,‡,§]

[†]Istituto Nanoscienze, Consiglio Nazionale Delle Ricerche (CNR), Via Arnesano, I-73100 Lecce, Italy

[‡]Center for Biomolecular Nanotechnologies @UNILE, Istituto Italiano di Tecnologia, Via Barsanti, I-73010 Arnesano LE, Italy

[§]Dipartimento di Matematica e Fisica "Ennio De Giorgi", Università del Salento, Via Arnesano I-73100 Lecce, Italy

Supporting Information

ABSTRACT: All-optical signal processing is the focus of much research aiming to obtain effective alternatives to existing data transmission platforms. Amplification of light in fiber optics, such as in Erbium-doped fiber amplifiers, is especially important for efficient signal transmission. However, the complex fabrication methods involving high-temperature processes performed in a highly pure environment slow the fabrication process and make amplified components expensive with respect to an ideal, high-throughput, room temperature production. Here, we report on near-infrared polymer fiber amplifiers working over a band of ∼20 nm. The fibers are cheap, spun with a process entirely carried out at room temperature, and shown to have amplified spontaneous emission with good gain coefficients and low levels of optical losses (a few cm^{-1}). The amplification process is favored by high fiber quality and low self-absorption. The found performance metrics appear to be suitable for short-distance operations, and the large variety of commercially available doping dyes might allow for effective multiwavelength operations by electrospun amplified fiber optics.

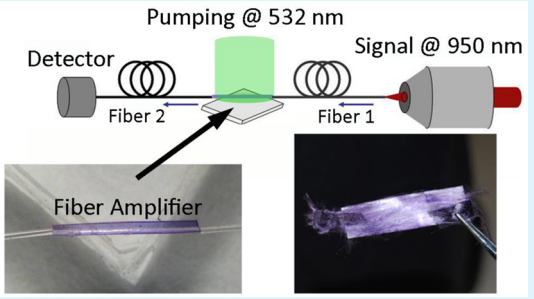

KEYWORDS: *electrospinning, optical gain, plastic optical amplifier, dye-doped fibers*

INTRODUCTION

In the information era, the capability of transmitting data in an efficient way represents the touchstone for establishing technological leadership.[1−3] In particular, yielding efficient transmission of optical data with minimal attenuation is a traditional challenge. These days, the preferred method is to use amplifiers that are able to counterbalance the intrinsic attenuation of transmission channels. Although silica fiber amplifiers doped by Erbium or other rare-earth ions[4−8] are generally used for long-distance operations, polymer fibers exhibiting optical gain can be advantageous for applications relying on short-range signal transmission with a large number of nodes, including domotics and biomedical networks. The operation of such fibers has hitherto been largely limited to the visible range.[9−12] In these components, the amplification process is promoted by stimulated emission occurring in chromophores or active dopants once population inversion is reached and a spectrally matching signal passes through the fibers. In this respect, an optical amplifier can be considered as a lasing system that lacks feedback.

In a typical working architecture, one end of a fiber or waveguide is doubly coupled, namely, it is interfaced to both the transmission line and pumping source, the latter of which leads to the population inversion.[9−12] A number of processes, such as self-absorption by the active materials and out-coupled light at the fiber surface, contribute to optical losses, which limit the system's efficiency. In addition, spurious spontaneous emission is a common source of noise because the produced light does not have coherence characteristics as required for amplification. Moreover, spontaneous emission could in turn be amplified once population inversion is reached, thus competing with the main signal.

In this framework, most of the silica-based systems present a drawback based on the complexity of their fabrication, which may involve vapor deposition techniques or quite complex chemical methods, interfacial gel polymerization, preforming, and so forth. Such processes may require a highly pure environment and may be slow or generally expensive. Polymeric systems, on the other hand, can be valuable alternatives for many applications in industrial automation and multimedia connections in cars.[13,14] Plastic materials are advantageous based on the wide versatility of available doping compounds and molecular dyes, making them appealing for the development of all-optical amplification schemes.[15] In addition, it should be mentioned that coupling miniaturized fibers with conventional fiber optics is often problematic.[2] However, efficient evanescent coupling with tapered optical fibers has been recently been used to successfully couple a variety of glass, polymer, and miniaturized metal fibers.[16,17] For all of these reasons, the achievement of alternative, low-cost, versatile amplified fibers that allow different experimental configurations to be developed is highly desired.

Over the past two decades, organic gain media have attracted great interest as light-emitting sources, lasers, and optical

Received: November 17, 2014
Accepted: February 9, 2015
Published: February 24, 2015

DOI: 10.1021/am508046g
ACS Appl. Mater. Interfaces 2015, 7, 5213−5218

amplifiers.[2,18] Drawn and spun active nanofibers,[3,19] have recently emerged as building blocks for photonics as they exhibit all the advantages of organics, including the low cost of materials and processing, the simplicity of their fabrication methods, as well as the possibility to engineer their optical properties, photoluminescence quantum yield, and Stokes shift.[20] These fibers are also fully compatible with dyes,[9,15] rare-earth ions,[21,22] and nanocrystal dopants.[22−24] Furthermore, fibrous organic amplifiers may show a large stimulated emission cross-section, which makes them attractive for optical sensing, on-chip spectroscopy, data communications, and processing,[18] including light amplification and logic operations. In particular, electrospinning is a low-cost, high-throughput, room-temperature process for making fibers.[25] Hence, electrospun fiber optics present clear advantages, including low power consumption for their production as well as for their operation due to their low thresholds for optical gain and their high fluorescence efficiency.[20]

Here, we report on near-infrared (NIR) amplifiers, based on individual, electrospun plastic fibers with lengths up to several mm, and on their arrays. We focus on molecular systems that emit at wavelengths around the first transmission window of conventional optical fibers. Furthermore, the NIR region (wavelengths ≤950 nm) is also of interest for many biomedical applications, such as in vivo fluorescence imaging and sensing, due to the low autofluorescence of biological tissues and deep penetration under human skin.[26−28] The system proposed here shows an amplification of 14 dB over a length of 8 mm, and it works on a wavelength band of 20 nm around the peak at 950 nm with optical gain and loss metrics that are good compared to those of other microfabricated polymer fibers.[9−12]

RESULTS AND DISCUSSION

We electrospun poly(methyl methacrylate) (PMMA) doped with a 2-[2-[3-[[1,3-dihydro-1,1-dimethyl-3-(3-sulfopropyl)-2*H*-benz[*e*]indol-2-ylidene]ethylidene]-2-[4-(ethoxycarbonyl)-1-piperazinyl]-1-cyclopenten-1-yl]ethenyl]-1,1-dimethyl-3-(3-sulfopropyl)-1*H*-benz[*e*]indolium hydroxide, inner salt, compound and *N*,*N*-diethylethanamine (1:1) (hereafter referred to as IR 144). The basic spectral features of the emitting system are shown in Figure S1 in the Supporting Information, highlighting a 320 meV gap from the absorption maximum to the peak of the amplified spontaneous emission (ASE). Uniaxially aligned and randomly oriented fibers can be easily obtained by varying the geometry of the collecting surfaces in the electrospinning setup. Examples of aligned fibers are displayed in Figure 1a and b. The fibers may exhibit a ribbon shape, resulting from rapid solvent evaporation and consequent solidification of the jet surface followed by collapse of the formed sheath.[29] Such fibers feature cross-sectional dimensions that can range from the scale of 1 μm to (500 μm × 70 μm) (Figure S2a in the Supporting Information) depending on the process parameters. The IR 144 dye is uniformly distributed in the host matrix (Figure S2b in the Supporting Information). Figure 1c sketches the waveguiding properties of our fibers measured by microphotoluminescence (μ-PL) experiments. By exciting the fiber at a varying distance, D, from the exit termination, we observe some luminescence signal escaping the fiber body (the spots on the right in Figure 1c) and an emission guided along the fiber's longitudinal axis. The out-coupled signal from the fiber termination decreases by increasing the distance D, as highlighted by the vertical arrows in Figure 1c. Optical losses can be ascribed to a number of physical

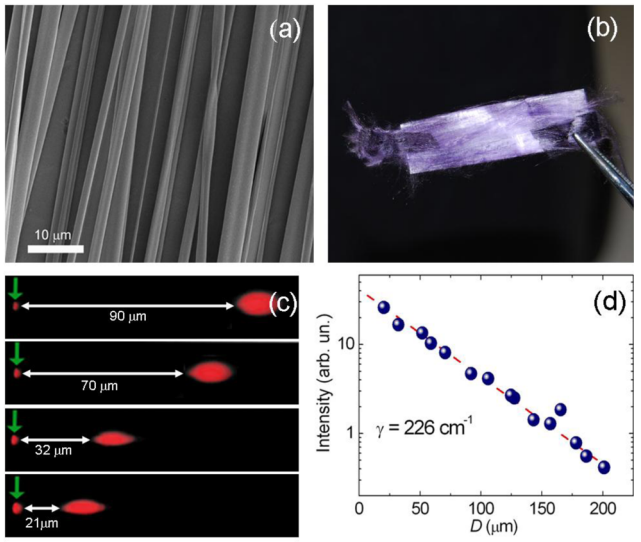

Figure 1. (a) Scanning electron micrograph of fibers doped with IR 144 and aligned in a bundle. Each individual fiber appears uniform along its length and is free of defects. (b) Photograph of a free-standing bundle of uniaxially aligned IR 144-based fibers. (c) Micrographs of IR 144-based fibers (μ-PL) pumped by a laser excitation beam tightly focused in spots (right, bright spots) at variable distances, D, from the fiber termination (left, smaller spots). This termination is highlighted by vertical arrows and corresponds to the point from which the out-coupled PL signal is collected after being transmitted along the fiber's longitudinal axis. (d) Corresponding PL intensity vs D (symbols) and best fit to the equation $I_{PL} = I_0 e^{-\gamma D}$ (dashed line).

mechanisms, such as residual self-absorption.[15] Analysis of the emitted intensity (I_{PL}) as a function of the tip-excitation distance (D) gives insight into the total losses (γ) in the fibers by fitting the experimental data by the expression $I_{PL} = I_0 e^{-\gamma D}$ (Figure 1d). We find $\gamma = (226 \pm 10)$ cm^{-1} for fibers under continuous wave excitation, a value in line with or outperforming electrospun polymer fibers with emission in the visible spectral range.[30]

We then investigated the gain properties in both bundles and single fibers and the amplification of transmitted optical signals by ASE experiments. Figure 2a displays the fiber emission spectra collected at different excitation fluences and pumping by a stripe along the alignment direction in the bundle.

The emission is peaked at ∼950 nm (Figure 2a) with minor spectral fluctuations as is typical of ASE. In particular, the intensity undergoes a rapid increase when optical pumping exceeds a value of ∼1.5 mJ/cm^2, and then follows a superlinear dependence trend (in the range 2−4 mJ/cm^2) until saturation is approached (at ∼5−6 mJ/cm^2, Figure 2b). Spontaneous emission stays low (Figure S3 in the Supporting Information), and the full width at half-maximum (fwhm) of the emission spectra decreases as a consequence of the amplification, reaching a value as low as 19 nm. ASE is a fundamentally thresholdless process;[31] however, an experimental threshold can be conventionally defined as the value of the excitation fluence at which the measured fwhm reaches the average of the fwhm of the spontaneous emission and that of ASE.[32] This approach provides a threshold excitation fluence of ∼2.5 mJ/cm^2 for IR 144-doped electrospun fibers. At fluences of 10−12 mJ/cm^2, photobleaching effects become significant and decreased ASE is observed (Figure S4 in the Supporting Information), whereas evidence of physical damage (laser

DOI: 10.1021/am508046g
ACS Appl. Mater. Interfaces 2015, 7, 5213−5218

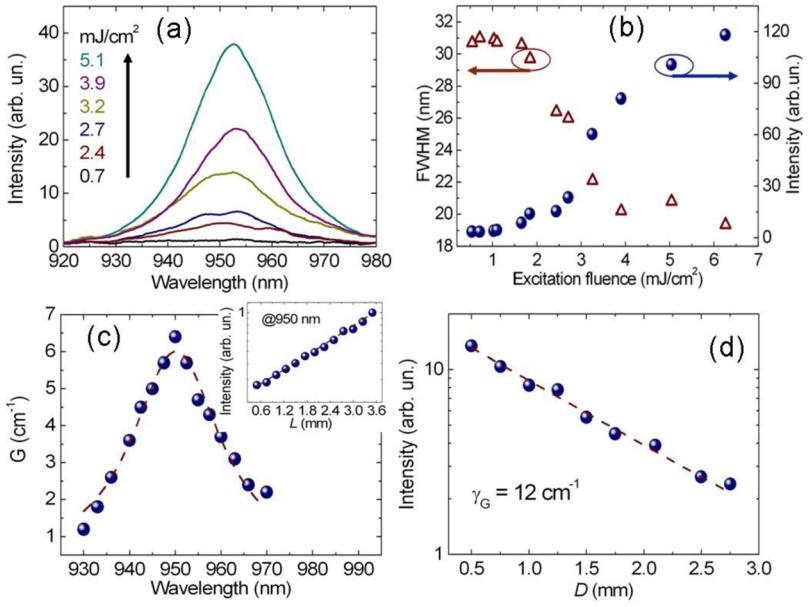

Figure 2. (a) ASE spectra from fibers for various excitation fluences. (b) ASE intensity (full symbols) and fwhm (empty symbols) vs excitation fluence. (c) Wavelength dependence of the net gain of fibers. The dashed line is a guide. Inset: net gain analysis performed at 950 nm. (d) Analysis of losses under pulsed excitation. Experimental values of the ASE intensity (symbols) are plotted vs. the distance of the exciting stripe from the emitting edge of the substrate. The dashed fitting line is obtained by the equation: $I_{PL} = I_0 e^{-\gamma_G D}$. In (c) and (d), the excitation fluence is 3.3 mJ/cm^2.

ablation) in fibers is found at fluences exceeding 40 mJ/cm^2. This class of ASE-showing spun fibers reveals interesting perspectives for signal transmission and amplification. In particular, if the transmitted signal wavelength matches that of the maximum material gain well, the amplification process could proceed in an efficient way. The efficiency basically depends on the pumping fluence and signal level[33,34] and is decreased by possible detrimental effects, such as noise and/or losses that deplete the excited states. Fibers based on four-level active molecular systems, for which the gain threshold and self-absorption are minimized (due to large Stokes shifts),[2,9,15] would be advantageous because they show minimal noisy emission.[2,5,9,15,18,31] We determined the wavelength dependence of the net gain, $G(\lambda)$, along our fibers by fitting the data of PL intensity (I_L) against the excitation stripe length (L) at each wavelength with the equation

$$I_L = \frac{I_p A(\lambda)}{G(\lambda)}[e^{G(\lambda)L} - 1] \quad (1)$$

where I_p represents the pump intensity and $A(\lambda)$ is a factor accounting for the spontaneous emission cross-section. The results are shown in Figure 2c and reveal a maximum G value of almost 7 cm^{-1} at a wavelength of 950 nm.

Optical losses under pulsed pumping conditions are determined by moving an excitation stripe of fixed length (4 mm) away from the emitting termination of fibers, thus increasing the separation distance D, namely, the length of the unexcited region. This experiment leads to the loss coefficient measurement $\gamma_G = (12 \pm 1)$ cm^{-1} (Figure 2d), a value much smaller than that obtained for the waveguided spontaneous emission (Figure 1d). This difference can be rationalized by considering that ASE (peaked at 950 nm) is affected by self-absorption losses that are lower than those of the spontaneous emission (peak at ~865 nm). This behavior can be taken into account by calculating the ratio of the absorption coefficients measured at the absorption (α_{abs}) and emission ($\alpha_{PL,ASE}$) peaks:[35] $S_{PL,ASE} = \alpha_{abs}/\alpha_{PL,ASE}$, where the PL and ASE subscripts indicate spontaneous emission and the ASE peak wavelength, respectively. Higher S values correspond to lower contribution of self-absorption to propagation losses. In our system, we find $S_{PL} = 3$ and $S_{ASE} = 35$, whose ratio (~12) is in good agreement with the measured ratio of loss coefficients, $\gamma/\gamma_G \cong 19$. The γ_G measured here is slightly higher than that found in visible-emitting conjugated polymer slabs made of poly(9,9-dioctylfluorene) or blends of poly(*p*-phenylenevinylene) derivatives.[36,37] Given the reduced size of the electrospun fibers and the relatively lower refractive index of PMMA compared to those of conjugated polymers (in principle, both features increase optical losses from waveguides), these results support the high surface quality, low density of light-scattering defects, and the reduced self-absorption of the microfabricated amplifiers generated here.

A simple proof-of-principle experiment can be based on a conservative approach in terms of amplifier working conditions with the aim of minimizing noisy signals and avoiding saturation effects without the need for pump−signal synchronization. We chose a non-monochromatic signal with a central wavelength corresponding to the maximum optical gain (at 950 nm) and a line width comparable to that of the fiber gain. The pumping fluence was chosen in the large range of superlinear variation of ASE intensity. Fibers are excited by a wavelength of 532 nm through a side-pump scheme based on a collimated, uniform pump beam (Figure 3).[38] Such a scheme substantially differs from configurations that are typically used in rare-earth-doped fiber lasers, such as the end-pump scheme and the more recently distributed side-coupled cladding-pumping scheme, which has been designed to avoid the high temperature rise occurring at the terminations of end-pumped, high-power fiber lasers.[39] The choice of a side pump scheme here is due to the high absorption coefficient of organic nanofibers compared to that of the rare-earth fiber lasers. Here, the dye absorption at the pumping wavelength (λ = 532 nm) is on the order of 10^6 dB/m, which is much higher than values in rare earth-doped

DOI: 10.1021/am508046g
ACS Appl. Mater. Interfaces 2015, 7, 5213−5218

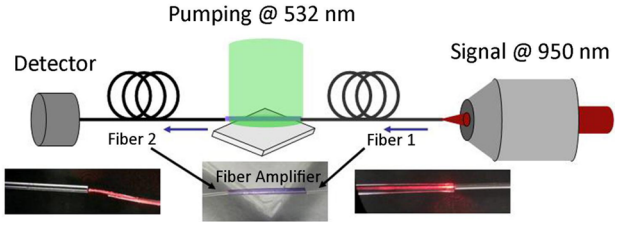

Figure 3. Experimental configuration of the electrospun fiber amplifier. The probe signal (at 950, 960, or 970 nm) is launched into a single mode fiber (fiber 1, core diameter of 6.6 μm) and passes through a single electrospun fiber deposited on a PDMS substrate to provide amplification. The signal is then coupled to a second optical fiber (fiber 2) and collected by a NIR detector. Pumping is performed by a collimated laser beam (λ = 532 nm). Photographs of a representative single electrospun fiber butt-coupled to fiber 1 and 2 are shown in the insets at the bottom.

fiber lasers that have pumping wavelengths on the order of 1−10^2 dB/m.[40,41] This high absorption would lead to substantial attenuation of the pumping beam within a depth of ∼20 μm in the plastic medium, which makes side-pump schemes more effective for electrospun fiber amplifiers. A single, active electrospun fiber is then deposited on a polydimethylsiloxane (PDMS) substrate and coupled to an input and output monomodal fiber in a butt-coupling configuration as shown in Figure 3. Figure 4 shows the resulting differential transmission, $\Delta T/T$, measured in a single fiber at different pump fluences (Figure 4a) and at different wavelengths (Figure 4b). For each data point, we recorded the intensity of four transmitted signals (I_{00}, I_{01}, I_{10}, and I_{11}). I_{00} corresponds to a configuration with both the pump and the input signal turned off, I_{01} to that with pump off and signal on, I_{10} to that with pump on and signal off, and I_{11} represents the transmitted intensity with both pump and signal on. The relative increase in the intensity of the transmitted signal, T, is then obtained by the ratio $(I_{11} - I_{10})/(I_{01} - I_{00})$[34] because $I_{11} - I_{10}$ is the transmitted signal intensity (T_F) at a given optical excitation density (i.e., at a given pump fluence), whereas $I_{01} - I_{00}$ represents the transmitted signal (T_0) in the absence of optical pumping. The differential transmission, ΔT, is consequently estimated as

$$\frac{\Delta T}{T} = \frac{T_F - T_0}{T_0} \quad (2)$$

Three regimes could be identified as featured by different transmission trends. Up to pumping fluences of ∼1−2 mJ/cm^2, the signal undergoes attenuation up to 4%, which can be related to photoinduced absorption phenomena leading to weaker transmission upon pumping. In the fluence range from 2 to 4 mJ/cm^2, the output signal increases with respect to the input, which is ascribable to the stimulated emission from IR 144 occurring at the signal wavelength (950 nm in Figure 4a). At fluences above 4 mJ/cm^2, the differential transmission remains unchanged, which is a fingerprint for the saturation of gain for which population inversion cannot be further enhanced, or decreases slightly analogous to the behavior found for ASE (Figure 2b). As further confirmation of the effective amplification process, we analyzed the signal transmission at 960 and 970 nm (Figure 4b), finding a lower gain in agreement with the spectrum obtained by the ASE characterization (Figure 2c). Importantly, amplification of ∼14 dB over a length of 8 mm is comparable to or larger than the typical maximum gain obtained in other dye-doped fiber amplifiers[12,38] as well as in rare-earth-doped fibers.[42] Considering their small size, these new fibrous systems can be considered as promising media for short-distance and pulsed amplification uses.

CONCLUSIONS

In conclusion, we demonstrate amplified fiber optics realized by electrospinning. Doped with NIR laser dyes, these plastic fibers allow optical amplification to be observed with good performances, including an operating range of 20 nm. They are flexible, lightweight, and capable of interfacing with conventional optical fibers, and they have unique fabrication advantages. These components are promising candidates for the future development of all-plastic, micro- to macroscale optical platforms for signal transmission and processing.

MATERIALS AND METHODS

Fiber Fabrication and Morphological Characterization. Bundles of uniaxially aligned fibers are fabricated by electrospinning a PMMA−IR 144 solution onto a rotating disk collector (diameter = 8 cm, thickness = 1 cm, 4000 rpm). Briefly, the solution is prepared by dissolving PMMA (375−650 mg/mL, depending on the desired final fiber thickness) with IR 144 (3.1 mg/mL) in chloroform and then sonicating at 40 °C for 6 h. The solution is loaded into a 1 mL syringe and delivered at a constant flow rate (1 mL/h) through a metal needle (21 gauge) connected to a high-voltage power supply (EL60R0.6−22, Glassman High Voltage, High Bridge, NJ). Upon applying voltage (10 kV), a polymer solution jet is ejected from the needle, and fibers are deposited on square (1 × 1 cm^2) quartz substrates mounted at the edge of the rotating disk. The morphology of the fibers is inspected using scanning electron microscopy (SEM, FEI, Hillsboro, OR) following thermal deposition of 5 nm of Cr. The average diameter of fibers is (1.8 ± 0.8) μm, calculated from SEM micrographs by imaging

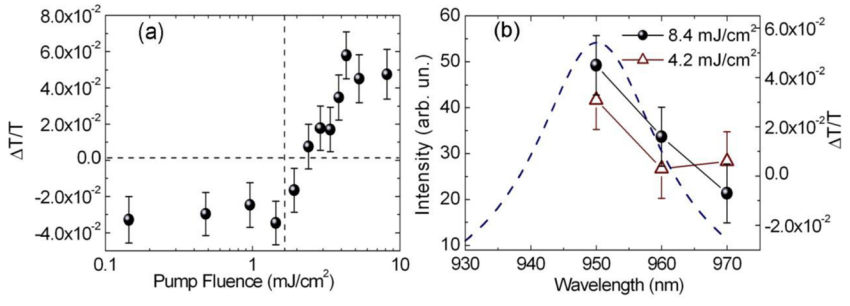

Figure 4. (a) Plot of the differential transmission along the electrospun fiber amplifier (at 950 nm) as a function of the excitation fluence. Net amplification of the transmitted signal is found at fluences larger than ∼2 mJ/cm^2. (b) Spectral dependence of the transmission at two distinct excitation fluences (full circles and empty triangles, right vertical scale) and gain spectrum (dashed line, left vertical scale). The maximum amplification is reached in correspondence to the maximum optical gain (Figure 2c).

DOI: 10.1021/am508046g
ACS Appl. Mater. Interfaces 2015, 7, 5213−5218

software (WSxM, Nanotec Electronica, Madrid, Spain) after analyzing at least 100 fibers.

Confocal and Waveguiding Measurements. Confocal micrographs (Olympus FV-1000) are collected by laser scanning (λ_{exc} = 405 nm) a field of fibers in epilayer configuration. The laser beam passes through an objective lens (40×, numerical aperture (NA) = 0.75) to impinge onto the fibers and excite fluorescence. The PL signal is then collected through the same microscope objective and analyzed by a multianode photomultiplier. A comprehensive description of waveguiding measurements by μ-PL is reported in ref 30. Briefly, the fibers are deposited on a quartz substrate and positioned in an inverted microscope. The fibers are cut, thus protruding from the substrate by ∼1 mm and suspended at one end. A laser beam (λ_{exc} = 408 nm) passes through an objective lens (20×, NA = 0.5) to excite the fibers, whose emission is then collected by the same objective, dispersed by a 0.33 m long monochromator and detected by a charge-coupled device (CCD). Alternatively, the fiber emission can be directed to another CCD camera (Leica, DFC 490) without spectral dispersion for imaging. The fibers are side-pumped at distance D from the freestanding tip. By varying the value of D, the PL intensity is measured relative to the distance, normalizing the data to the PL intensity collected from the excitation spot to account for local, minor sample disuniformities.

ASE Characterization. The fibers are put under vacuum and excited by the third harmonic of a pulsed Nd:YAG laser (λ_{exc} = 355 nm, repetition rate = 10 Hz, pulse duration = 10 ns). The excitation spot is focused on the samples in a stripe (maximum length = 4 mm), and the signal collected from one edge of the substrate is measured with a monochromator and a CCD. For net gain characterization, the stripe length is varied by a controllable slit while keeping the excitation fluence fixed. Optical losses under pulsed excitation conditions are investigated by varying the distance of the stripe from the fiber edge at a fixed fluence.

Transmission Measurements. For the input signal, the light from a halogen lamp is dispersed by a grating (600 lines/mm blazed at 1000 nm) to have an almost monochromatic beam with fwhm of ∼10 nm. To avoid saturation effects, the signal power density is kept low (a few watts per centimeter squared). The signal is passed through an objective lens (4×, NA = 0.16) and coupled to a single-mode optical fiber (core diameter = 6.6 μm, NA = 0.13). For the transmission measurements, a single electrospun fiber is butt-coupled to the input optical fiber at one end and to an identical optical fiber (output fiber) at the opposite end. The signal passing through the system is analyzed by a NIR, nitrogen-cooled CCD. The pump is provided by the second harmonic of a pulsed Nd:YAG laser (532 nm, repetition rate = 10 Hz, pulse duration = 10 ns) shaped to a uniform beam along the body of the electrospun amplifier. Measurements are performed by varying the pump fluence over more than 1 order of magnitude at values relevant to the stimulated emission dynamics.

■ ASSOCIATED CONTENT

Ⓢ Supporting Information

Spectral features of the emitting systems, single fiber morphology and fluorescence, and full spectral range emission characteristics. This material is available free of charge via the Internet at http://pubs.acs.org.

■ AUTHOR INFORMATION

Corresponding Author

*E-mail: dario.pisignano@unisalento.it.

Notes

The authors declare no competing financial interest.

■ ACKNOWLEDGMENTS

The authors thank Dr. P. Del Carro for help with the morphological characterization. This research received funding from the European Research Council under the European Union's Seventh Framework Programme (FP/2007-2013)/ERC Grant Agreement No. 306357 ("NANO-JETS").

■ REFERENCES

(1) Hoang, T. B.; Beetz, J.; Lermer, M.; Midolo, L.; Kamp, M.; Höfling, S.; Fiore, A. Widely Tunable, Efficient On-Chip Single Photon Sources at Telecommunication Wavelengths. *Opt. Express* **2012**, *20*, 21758−21765.

(2) Clark, J.; Lanzani, G. Organic Photonics for Communications. *Nat. Photonics* **2010**, *4*, 438−446.

(3) Wang, P.; Wang, Y.; Tong, L. Functionalized Polymer Nanofibers: A Versatile Platform for Manipulating Light at the Nanoscale. *Light: Sci. Appl.* **2013**, *2*, e102.

(4) Desurvire, E.; Simpson, J. R.; Becker, P. C. High-Gain Erbium-Doped Traveling-Wave Fiber Amplifier. *Opt. Lett.* **1987**, *12*, 888−890.

(5) Jackson, S. D. Towards High-Power Mid-Infrared Emission from a Fibre Laser. *Nat. Photonics* **2012**, *6*, 423−431.

(6) Tengattini, A.; Gandolfi, D.; Prtljaga, N.; Anopchenko, A.; Ramírez, J. M.; Ferrarese Lupi, F.; Berencén, Y.; Navarro-Urrios, D.; Rivallin, P.; Surana, K.; Garrido, B.; Fedeli, J.-M.; Pavesi, L. Toward a 1.54 μm Electrically Driven Erbium-Doped Silicon Slot Waveguide and Optical Amplifier. *J. Lightwave Technol.* **2013**, *31*, 391−397.

(7) Wei, T.; Chen, F.; Tian, Y.; Xu, S. Broadband Near-Infrared Emission Property in Er^{3+}/Ce^{3+} Co-Doped Silica−Germanate Glass for Fiber Amplifier. *Spectrochim. Acta, Part A* **2014**, *126*, 53−58.

(8) Foster, M. A.; Turner, A. C.; Sharping, J. E.; Schmidt, B. S.; Lipson, M.; Gaeta, A. L. Broad-Band Optical Parametric Gain on a Silicon Photonic Chip. *Nature* **2006**, *441*, 960−963.

(9) Arrue, J.; Jiménez, F.; Ayesta, I.; Illarramendi, M. A.; Zubia, J. Polymer-Optical-Fiber Lasers and Amplifiers Doped with Organic Dyes. *Polymers* **2011**, *3*, 1162−1180.

(10) Tagaya, A.; Koike, Y.; Kinoshita, T.; Nihei, E.; Yamamoto, T.; Sasaki, K. Polymer Optical Fiber Amplifier. *Appl. Phys. Lett.* **1993**, *53*, 883−884.

(11) Rajesh, M.; Sheeba, M.; Geetha, K.; Vallaban, C. P. G.; Radhakrishnan, P.; Nampoori, V. P. M. Fabrication and Characterization of Dye-Doped Polymer Optical Fiber as a Light Amplifier. *Appl. Opt.* **2007**, *46*, 106−112.

(12) Tagaya, A.; Teramoto, S.; Yamamoto, T.; Fujii, K.; Nihei, E.; Koike, Y.; Sasaki, K. Theoretical and Experimental Investigation of Rhodamine B-Doped Polymer Optical Fiber Amplifiers. *IEEE J. Quantum Electron.* **1995**, *31*, 2215−2219.

(13) Polishuk, P. Plastic Optical Fibers Branch Out. *IEEE Communications Magazine* **2006**, *9*, 140−148.

(14) Xia, R.; Cheung, C.; Ruseckas, A.; Amarasinghe, D.; Samuel, I. D. W.; Bradley, D. D. C. Wavelength Conversion from Silica to Polymer Optical Fibre Communication Wavelengths via Ultrafast Optical Gain Switching in a Distributed Feedback Polymer Laser. *Adv. Mater.* **2007**, *19*, 4054−4057.

(15) Morello, G.; Moffa, M.; Girardo, S.; Camposeo, A.; Pisignano, D. Optical Gain in the Near Infrared by Light-Emitting Electrospun Fibers. *Adv. Funct. Mater.* **2014**, *24*, 5225−5231.

(16) Gu, F. X.; Zhang, L.; Yin, X. F.; Tong, L. M. Polymer Single-Nanowire Optical Sensors. *Nano Lett.* **2008**, *8*, 2757−2761.

(17) Gu, F. X.; Yu, H. K.; Wang, P.; Yang, Z. Y.; Tong, L. M. Light-Emitting Polymer Single Nanofibers via Waveguiding Excitation. *ACS Nano* **2010**, *4*, 5332−5338.

(18) Samuel, I. D. W.; Turnbull, G. A. Organic Semiconductor Lasers. *Chem. Rev.* **2007**, *107*, 1272−1295.

(19) Camposeo, A.; Persano, L.; Pisignano, D. Light-Emitting Electrospun Nanofibers for Nanophotonics and Optoelectronics. *Macromol. Mater. Eng.* **2013**, *298*, 487−503.

(20) Morello, G.; Polini, A.; Girardo, S.; Camposeo, A.; Pisignano, D. Enhanced Emission Efficiency in Electrospun Polyfluorene Copolymer Fibers. *Appl. Phys. Lett.* **2013**, *102*, 111911−111915.

(21) Sun, X.; Li, B.; Song, L.; Gong, J.; Zhang, L. Electrospinning Preparation and Photophysical Properties of One-Dimensional (1D) Composite Nanofibers Doped with Erbium (III) Complexes. *J. Lumin.* **2010**, *130*, 1343−1348.

DOI: 10.1021/am508046g
ACS Appl. Mater. Interfaces 2015, 7, 5213−5218

(22) Zhao, P.; Zhang, M.; Wang, T.; Liu, X.; Zhai, X.; Qin, G.; Qin, W.; Wang, F.; Zhang, D. Optical Amplification at 1525 nm in $BaYF_5$: 20% Yb^{3+}, 2% Er^{3+} Nanocrystals Doped SU-8 Polymer Waveguide. *J. Nanomater.* **2014**, *2014*, 153028-1−153028-6.
(23) Yu, H. C. Y.; Argyros, A.; Barton, G.; van Eijkelenborg, M. A.; Barbe, C.; Finnie, K.; Kong, L.; Ladouceur, F.; McNiven, S. Quantum Dot and Silica Nanoparticle Doped Polymer Optical Fibers. *Opt. Express* **2007**, *15*, 9989−9994.
(24) Liu, H.; Edel, J. B.; Bellan, L. M.; Craighead, H. G. Electrospun Polymer Nanofibers as Subwavelength Optical Waveguides Incorporating Quantum Dots. *Small* **2006**, *2*, 495−499.
(25) Camposeo, A.; Di Benedetto, F.; Stabile, R.; Neves, A. A. R.; Cingolani, R.; Pisignano, D. Laser Emission from Electrospun Polymer Nanofibers. *Small* **2009**, *5*, 562−566.
(26) Weissleder, R. A Clearer Vision for in Vivo Imaging. *Nat. Biotechnol.* **2001**, *19*, 316−317.
(27) Leevy, W. M.; Gammon, S. T.; Jiang, H.; Johnson, J. R.; Maxwell, D. J.; Jackson, E. N.; Marquez, M.; Piwnica-Worms, D.; Smith, B. D. Optical Imaging of Bacterial Infection in Living Mice Using a Fluorescent Near-Infrared Molecular Probe. *J. Am. Chem. Soc.* **2006**, *128*, 16476−16477.
(28) Kobayashi, H.; Ogawa, M.; Alford, R.; Choyke, P. L.; Urano, Y. New Strategies for Fluorescent Probe Design in Medical Diagnostic Imaging. *Chem. Rev.* **2010**, *110*, 2620−2640.
(29) Koomhongse, S.; Liu, W.; Reneker, D. H. Flat Polymer Ribbons and Other Shapes by Electrospinning. *J. Polym. Sci., Part B: Polym. Phys.* **2001**, *39*, 2598−2606.
(30) Fasano, V.; Polini, A.; Morello, G.; Moffa, M.; Camposeo, A.; Pisignano, D. Bright Light Emission and Waveguiding in Conjugated Polymer Nanofibers Electrospun from Organic Salt Added Solutions. *Macromolecules* **2013**, *46*, 5935−5942.
(31) Svelto, O. *Principles of Lasers*, 4th ed; Springer: New York, 1998.
(32) Ichikawa, M.; Hibino, R.; Inoue, M.; Haritani, T.; Hotta, S.; Koyama, T.; Taniguchi, Y. Improved Crystal-Growth and Emission Gain-Narrowing of Thiophene/Phenylene Co-Olygomers. *Adv. Mater.* **2003**, *15*, 213−217.
(33) Amarasinghe, D.; Ruseckas, A.; Vasdekis, A. E.; Turnbull, G. A.; Samuel, I. D. W. High-Gain Broadband Solid-State Optical Amplifier using a Semiconducting Copolymer. *Adv. Mater.* **2009**, *21*, 107−110.
(34) Dal Negro, L.; Cazzanelli, M.; Danese, B.; Pavesi, L.; Iacona, F.; Franzò, G.; Priolo, F. Light Amplification in Silicon Nanocrystals by Pump and Probe Transmission Measurements. *J. Appl. Phys.* **2004**, *96*, 5749−5755.
(35) Currie, M. J.; Mapel, J. K.; Heidel, T. D.; Goffri, S.; Baldo, M. A. High-Efficiency Organic Solar Concentrators for Photovoltaics. *Science* **2008**, *321*, 226−228.
(36) McGehee, M. D.; Gupta, R.; Veenstra, S.; Miller, E. K.; Diaz-Garcia, M. A.; Heeger, A. J. Amplified Spontaneous Emission from Photopumped Films of a Conjugated Polymer. *Phys. Rev. B* **1998**, *58*, 7035−7039.
(37) Heliotis, G.; Bradley, D. D. C.; Turnbull, G. A.; Samuel, I. D. W. Light Amplification and Gain in Polyfluorene Waveguides. *Appl. Phys. Lett.* **2002**, *81*, 415−417.
(38) Maier, G. V.; Kopylova, T. N.; Svetlichnyi, V. A.; Podgaetskii, V. M.; Dolotov, S. M.; Ponomareva, O. V.; Monich, A. E.; Monich, E. A. Active Polymer Fibres Doped with Organic Dyes: Generation and Amplification of Coherent Radiation. *Quantum Electron.* **2007**, *37*, 53−59.
(39) Huang, Z.; Cao, J.; Guo, S.; Chen, J.; Xu, X. Comparison of Fiber Lasers Based on Distributed Side-Coupled Cladding-Pumped Fibers and Double-Cladding Fibers. *Appl. Opt.* **2014**, *53*, 2187−2195.
(40) Jeong, Y.; Sahu, J.; Payne, D.; Nilsson, J. Ytterbium-Doped Large-Core Fiber Laser with 1.36 kW Continuous-Wave Output Power. *Opt. Express* **2004**, *12*, 6088−6092.
(41) Data on commercially available Er-doped fibers can be found at www.thorlabs.com.
(42) Anthony, R.; Lahiri, R.; Biswas, S. An L-Band-Cascaded Erbium-Doped Fiber Amplifier for Uniform Gain without Equalizing Filter. *Microwave and Optical Technology Letters* **2014**, *56*, 2053−2055.

DOI: 10.1021/am508046g
ACS Appl. Mater. Interfaces 2015, 7, 5213−5218